Digest Journal of Nanomaterials and Biostructures Vol. 9, No. 3, July – September 2014, p. 1125 - 1135

MICROSTRUCTURAL PARAMETERS EVALUATION OF RF SPUTTERED TiO_2 THIN FILM ON VARIOUS SUBSTRATES

S. SHANMUGAN[a*], D. MUTHARASUa, I. Abdul Razak[b]
[a]*Nano Optoelectronics Research Laboratory, School of Physics,*
UniversitiSains Malaysia (USM), 11800, Minden, Pulau Pinang, Malaysia.
[b]*X-ray Crystallography Laboratory, School of Physics,*
UniversitiSains Malaysia (USM), 11800, Minden, Pulau Pinang, Malaysia.

Titanium Oxide (TiO_2) thin film was deposited on glass and Al substrates using Radio Frequency sputtering and studied their structural properties using XRD spectra. Mixed phases (Orthorhombic &Tetragonal) were observed on both substrates when the samples are annealed at lower temperatures (≤ 200°C). A preferred orthorhombic phase was observed on glass substrates whereas tetragonal phases was exist on Al substrates at higher annealing temperatures (≥ 300°C). Microstructural parameters such as residual stress, micro-strain, texture coefficient, crystallite size and dislocation density were evaluated form the XRD spectra and observed noticeable variation with respect to the crystal orientation of TiO_2 thin film exist at various annealing temperatures. Considerable change in structural parameters was observed for the film annealed at 100°C. Tensile stress was noticed for TiO_2 thin film on glass substrates while compressive stress observed for TiO_2 on Al substrates.

(Received July 10, 2014; Accepted September 15, 2014)

Keywords: TiO_2 thin film, XRD analysis, microstructural parameters, residual stress,

1. Introduction

Titanium oxide (TiO_2) is one of the most important functional semiconductor materials. Among metal oxide nano structures, TiO_2 offers a range of physical and chemical properties that make it suitable for a wide spectrum of applications. Its semiconductor properties also make it a suitable electrode material for the conversion of light energy into electrical energy. It is transparent to visible light, has high refractive index and excellent chemical stability over a wide pH range and in alarge number of solvents [1]. TiO_2-films could become valuable light emitting materials if they are doped with highly luminescent rare earth ions [2-4]. There are three different crystalline phases of TiO_2, namely anatase, rutile, and brookite [5]. In addition, amorphous TiO_2 films are often observed when deposition temperature is low. Depending on the phase structure, the TiO_2 films can be tailored for different applications. So it is necessary to understand the phase structure of TiO_2 when it is deposited on different substrates. Normally, the TiO_2 thin film was deposited on Si substrates for semiconductor applications [6]. Many research works have been focused on metal substrate for TiO_2 thin film [7], [8] and [9]. Even though, the TiO_2 thin film have been deposited on various metal substrates, such as stainless steel [10], Ni [11] and most of the research papers are dealt only in the study of the crystal structure of TiO_2 film, the catalytic reaction, etc. However, not many works have been undertaken to estimate the structural parameters such as stress, internal strain, dislocation density etc., with respect to their orientations. It will be very useful to decide the material for suitable application especially mechanical.

TiO_2 thin films can be prepared by various techniques such as sol-gel, chemical vapor deposition, pulsed laser deposition or sputtering. Experimental results have shown that the preparation technique and processing conditions have a strong influence on the microstructure and

---

[*] Corresponding author: shagan77in@yahoo.co.in

physical properties of the material. Each of these methods has its own advantages and limitations [12]. Among the available preparation techniques, Reactive rf sputtering is widely used to prepare Ti compound thin films such as TiO_2 and TiN [13]. In this work, TiO_2 thin film was prepared on various substrates by rf sputtering and studied their structural parameters by using XRD spectra.

2. Experimental methodology

TiO_2 thin films were deposited on glass (7.5 x 2.5 cm) and Al substrates (2.3 cm x 2.5 cm) using TiO_2 (99.99% purity) target (3 inch in diameter and 4 mm in thickness) in the presence of high pure Ar (99.999%) by RF sputtering (Edwards make, Model-Auto 500). Before we load the substrates, they were cleaned by rinsing in ultrasonic bath contains acetone and isopropyl alcohol. Initially, the sputtering system was pumped down to 2.6×10^{-6} mbar and loaded the sputtering target and substrates by venting the chamber. Later the deposition chamber was evacuated to 3.5×10^{-3} mbar (sputtering pressure) and all thin film coating was performed at 0.6 Å / sec deposition rate. Before the TiO_2 thin film deposition, pre-sputtering was carried out for about 5 min at Ar pressure of 3.5×10^{-3} mbar and expected to remove the surface oxidation of the target. 150W RF power was used to sputter the TiO_2 target and achieved 300 nm thickness recorded by digital thickness monitor during the TiO_2 thin film deposition. The substrate to target distance was fixed at 7 cm. After thin film preparation, the samples were annealed at various temperatures from 100 to 400 °C (100 °C step) for about 1 hr in CVD tube furnace. For easy discussion, the as grown film is mentioned as the annealing temperature at 25°C throughout this manuscript.

The processed samples were tested for their structural parameters by X-ray Diffraction technique (XRD-Siemens diffractometer D5000) and the structural parameters such as micro-strain, dislocation density, crystallite size, internal stress and texture coefficient were evaluated and discussed here.

3. Results and discussions

3.1 XRD Spectra analysis

The XRD spectra of TiO_2 thin film were recorded for various annealing temperatures as shown in fig.1 & fig. 2. The observed and standard 2θ and d space values for TiO_2 thin film deposited on glass and Al substrates are compared and the values are given in Table – 1 and 2. Fig. 1 shows the XRD spectra of annealed TiO_2 thin film deposited on glass substrates and shows the amorphous structure when the sample annealed at upto 200 °C [14]. In addition, TiO_2 thin film annealed at 300°C shows polycrystalline nature as the presence of tetragonal and orthorhombic phases. It is clearly visible that the tetragonal peaks are disappear when the sample annealed at 400°C and exist with only orthorhombic phases. For TiO_2 on Al, the XRD spectra of TiO_2 thin films annealed at various temperatures were recorded as shown in fig. 2. It clearly indicates the presence of polycrystalline TiO_2 for various temperatures [15].

Table 1. Structural properties of TiO_2 thin film on glass substrates for various annealing temperatures.

2θ (O)	2 θ (S)	FWHM	*d* space (O)	*d* space (S)	Residual stress (GPa)	Phase
300°C						
27.49	27.33	0.1574	3.245	3.260	1.033	T
31.77	31.38	0.0960	2.815	2.848	2.650	O
56.59	56.39	0.0720	1.625	1.630	0.759	T
66.34	66.9	0.0960	1.408	1.397	-1.738	O
400°C						
31.77	31.38	0.0960	2.815	2.848	2.758	O
66.32	66.9	0.0720	1.407	1.397	-1.784	O

(O) – observed, (S) – Standard

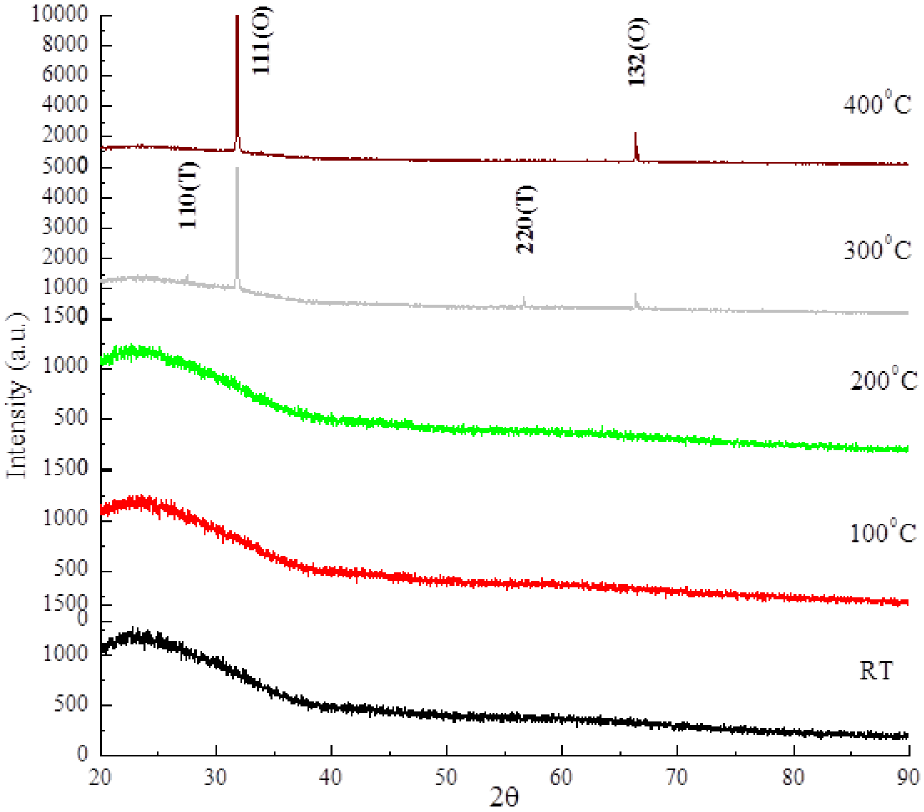

Fig.1. XRD spectra of rf sputtered TiO_2 thin film on glass substrates for various annealing temperatures

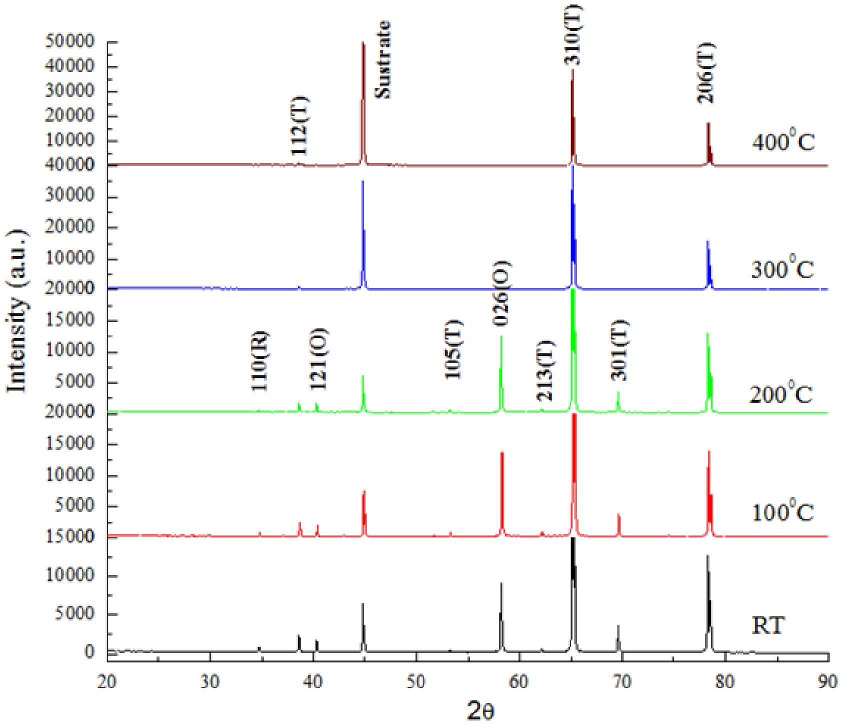

Fig.2. XRD spectra of rf sputtered TiO_2 thin film on Al substrates for various annealing temperatures

In addition, it is visible from the fig.2 that the intensities were high for high annealing temperature. It represents the improved crystallinity of TiO_2 thin film at high annealing temperature. From fig.2, XRD spectra of the film annealed at upto 200°C shows the presence of mixed phases (Orthorhombic, Tetragonal and Rhombohedral) with different peak intensities. Among these phases, tetragonal is preferentially oriented than other phases and orthorhombic phases are next to tetragonal phases when the TiO_2 thin films are annealed at upto 200°C. From the fig.2, it is also confirmed that the trace amount of rhombohedral (110) phase is observed for annealing temperature at upto 200°C. The peaks related to orthorhombic phases with (026) orientation are also observed with high intensities along with tetragonal phases which are also disappear when the sample annealed at above 300°C.

Fig.2 also reveals that the stable TiO_2 phase (anatase) is possible on Al substrates when TiO_2 is annealed at higher temperatures (> 200°C) and there are no phases observed other than tetragonal phase [14]. In addition to the disappearance of orthorhombic and rhombohedral, few peaks of TiO_2 related to (105), (213) and (301) orientations are also disappear at higher annealing temperatures. From the fig. 1 and 2, at 400°C annealing temperature, the XRD spectra of TiO_2 prepared on glass substrates shows only orthorhombic phases but, which prepared on Al substrates show only tetragonal phases. It evidences the influence of substrates on the growth of TiO_2 with particular phase.

3.2 Peak intensity analysis

The XRD spectra of TiO_2 thin film deposited on glass and Al substrates show the formation of various phases with different orientations and showed the influence of substrates on the growth of TiO_2 thin film on particular phase. To understand clearly, the peak intensity analysis is also performed for all TiO_2 thin film samples. Fig. 1 shows that the noticeable change in the intensity of the peaks is observed at 31.77° and 66.32° respectively for TiO_2 on glass samples. It clearly indicates the presence of doublet peak (not shown) at the same range with small change in 2θ value. This is because of instrumental error i.e., unable to separate $K_{\alpha 1}$ and $K_{\alpha 2}$ radiation. The separation between the two peaks increases with increasing diffraction angle [16].

Consequently, the observed peak intensities of various orientations at different annealing temperatures for TiO_2 thin film on Al substrate are plotted in fig.3. It clearly depicts the influence of annealing temperature on peak intensity of TiO_2 thin film phases with various orientations. Overall, a noticeable change in intensity could be observed for the samples annealed at 100°C expect to (110) orientations. It agrees with the observation made for all other parameters. It is also observed that the peak intensity for all orientations decreases other than (213) orientation when the samples are annealed at 200°C. In addition, the peak intensity for (112) orientation decreases as the annealing temperature increases. This may be due to crystal defects at this particular orientation for higher annealing temperatures.

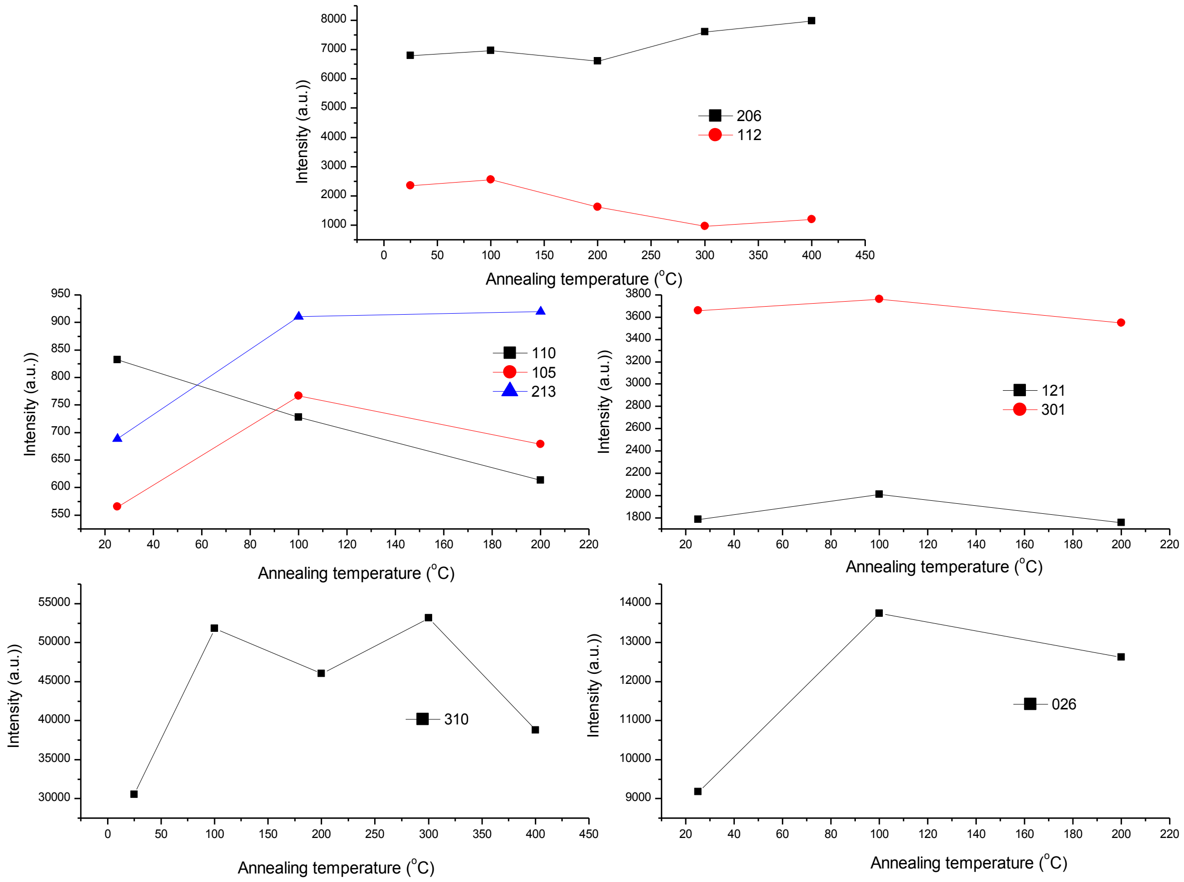

Fig.3. Change in intensity of various phases observed on TiO_2 thin film deposited on Al for different annealing temperatures.

3.3 Crystallite size analysis

The average crystallite sizes of TiO_2 thin film deposited on glass and Al substrates were calculated using Debye - Sherrer's equation as follows [17]:

$$D=0.9\lambda/\beta\cos\theta \tag{1}$$

Where λ is the wavelength of X-ray, β is the full-width at half-maximum (FWHM) of the peak (in radian), and the θ is the Bragg's angle of the X-ray diffraction peaks. The crystallite size of TiO_2 crystals was evaluated from the XRD data and plotted for observed crystal orientation against the annealing temperatures as shown in fig. 4. It clearly shows that a noticeable increment in crystallite size is observed for all orientation other than (206) and (121) orientation when the samples annealed at 100°C especially for (105) orientation. It is also observed that a high value and low value in crystallite size could be observed for (110) and (026) orientations respectively. A considerable reduction in crystallite size is also observed for higher annealing temperatures (> 100°C). There is no change in crystallite size for (310), (112) and (206) orientations even the annealing temperature increases (from 300 to 400°C).

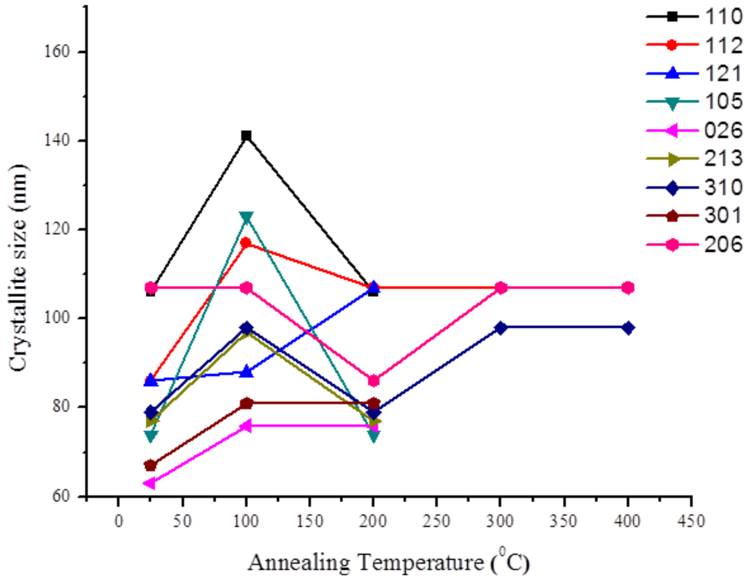

Fig.4. Variation in crystallite size of TiO_2 thin film on Al substrates at different annealing temperatures.

There is no much difference on crystallite size when TiO_2 on glass substrates annealed at above 300°C. Overall, the average crystallite size of the TiO_2 thin film increases for the film deposited on Al substrate for 300°C and decreases for 400°C.

3.4 Dislocation density analysis

In addition to the crystallite size of the TiO_2 on Al substrate, the dislocation density available in the TiO_2 crystal is also characterized and calculated from the formula [18];

$$\delta = 1/D^2 \tag{2}$$

Where D is the crystallite size of TiO_2 thin film and the calculated results are plotted for various orientations against the annealing temperatures as shown in fig.5. Since, the dislocation density is directly related to crystallite size, there is a correlation between crystallite size and dislocation density (see. equation 2). It clearly indicates that the dislocation density decreases noticeable for all orientations other than (206) and (121) orientations at 100°C and considerable increase in dislocation density is also observed for (213), (110), (206) and (310) orientations. From this observations, the samples annealed at 100°C show an immense effect on reducing the dislocation density for the crystals with (110), (301), (213) orientations especially for (105) orientation. As observed for crystallite size at higher annealing temperature, the dislocation density is not changing much for (310), (206) and (112) orientations when the annealing temperature increases from 300 to 400°C. From the fig.5, a high value in dislocation density is observed with (026) orientations than that of other orientations for as prepared samples. In addition, low value in dislocation density is also observed for (110) oriented crystals at 100°C.

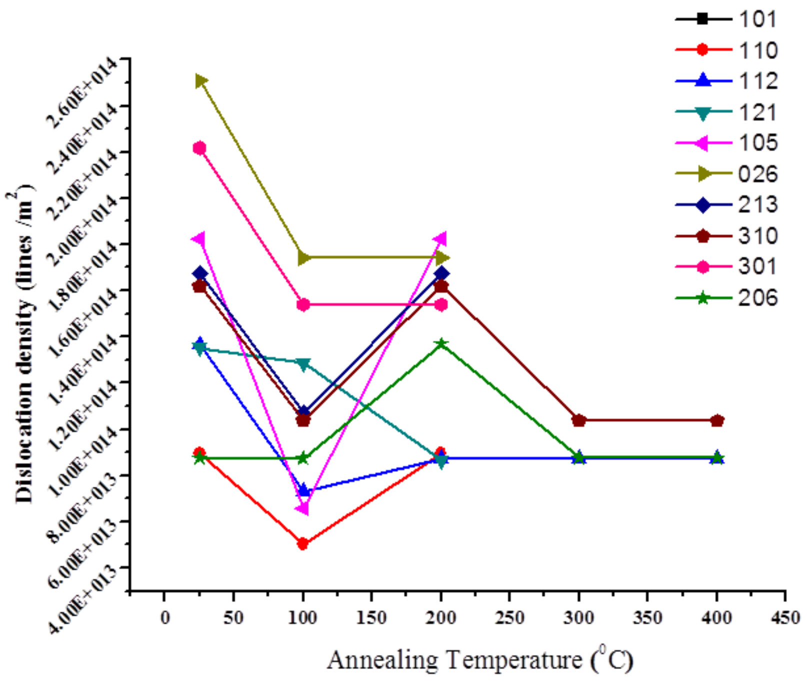

Fig.5. Variation in dislocation density of TiO_2 thin film on Al substrates at different annealing temperatures.

3.5 Strain analysis

In thin film application, the strain is important parameter and should be considered for testing which decides the mechanical properties of the thin film for desired application. To test the strain developed depends on various substrates, the following equation is used to measure the strain [19]:

$$\varepsilon=\beta\cos\theta/4 \quad (3)$$

Where β is FWHM and θ is diffraction angle in radian. The strain developed in the prepared TiO_2 thin film on Al substrates for various temperatures are plotted in fig.6 and shows the change in stress with respect to different orientations present in the prepared thin film. It clearly indicates that the orthorhombic phase with (121) orientations shows high value in strain than all other orientations in the prepared TiO_2 thin film. But it is also observed that a low value in strain is noticed with tetragonal phase with (206) orientation. As we observed for crystallite size and dislocation density, the strain value also obey the pattern and a noticeable decrease in strain value could be observed for all orientations other than (206) and (121) when the film annealed at 100°C.

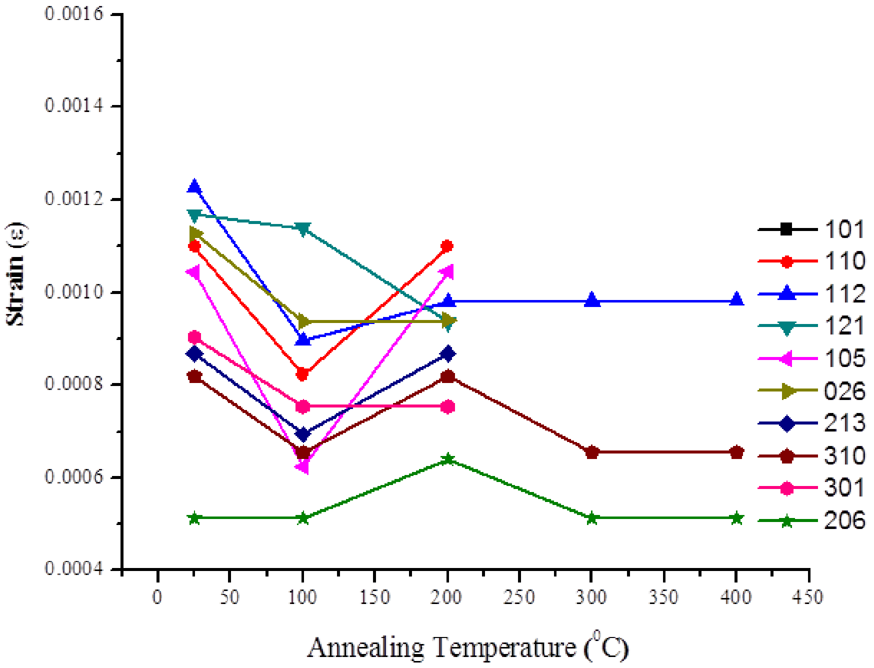

Fig.6. Variation in microstrain of TiO_2 thin film on Al substrates at different annealing temperatures.

3.6 Texture coefficient (TC) analysis

In order to study the preferred orientation of the crystals growth, the *TC* was evaluated for all samples using the formula given in equation (4) as follows [20]:

$$P_i\ (TC) = N\,(I_i/I_o)/\sum (I_i/I_o) \tag{4}$$

Where P_i is the Texture Coefficient of the plane *I*, I_i is the measured intensity, I_o is the intensity of the JCPDS powder diffraction pattern of the corresponding peak and *N* is the number of reflections considered for the analysis. When P_i is greater than unity, it is indicating that the peak is preferred orientation of the crystallites in that particular direction.

From the *TC* analysis, it is observed that the orthorhombic phases with (111) orientation are preferentially grown on the glass substrates when the sample annealed at above 300 °C. The *TC* analysis is also performed for TiO_2 thin film on Al substrates annealed at various temperatures. The calculated *TC* values are plotted for various orientations against the annealing temperature as shown in fig. 7 (a&b) and clearly indicates that the (310) orientation show high value for all temperature and observed as preferred growth on Al substrates. In addition, at below 200°C, TiO_2 thin film grow with (026) orientation as preferred on Al substrates than other orientations (see fig. 7b). Overall, the TiO_2 thin film with (026) orientations are expected to grow as preferred growth orientations on Al substrates.

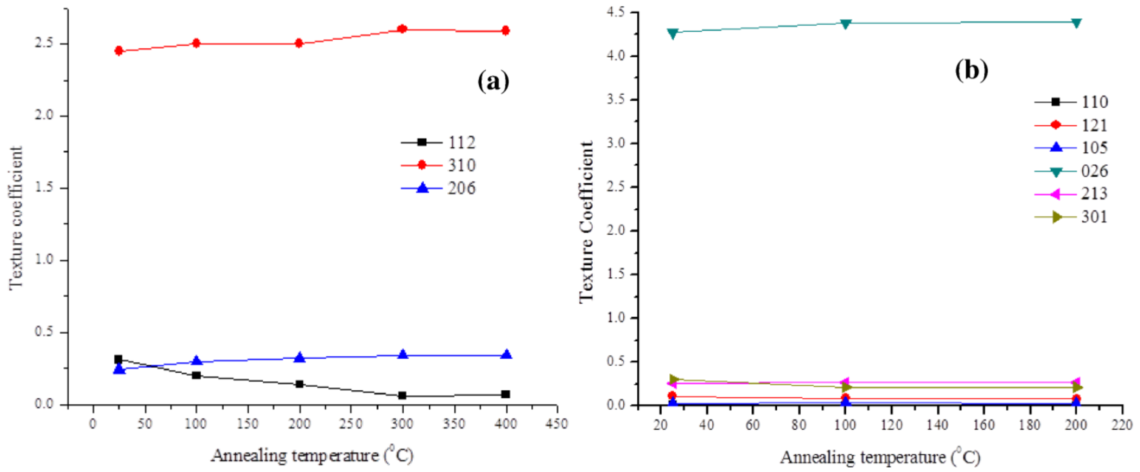

Fig.7. Change in Texture coefficient of various phases (a) (112), (310) & (206) and (b) (110), (121), (105), (026), (213) & (301) observed from TiO_2 thin film on Al substrates at different annealing temperatures.

3.7 Residual stress analysis

During the crystal growth, there may be possible for developing the stress as a result of growth temperature. In crystal, the residual stress is one which remains in material without application of an external load. Usually it originates during manufacturing and processing of materials due to heterogeneous plastic deformations, thermal contractions and phase transformations. Since our studies showed several phase transformation, it is necessary to study the residual stress of TiO_2 when it is deposited on various substrates. It is also evaluated using the following equation [21] ;

$$\sigma = -E(d_a - d_o)/(2d_o Y) \qquad (5)$$

where E and Y are the Young's modulus (157GPa) and the Poisson's ratio (0.35) of TiO_2 respectively [22]. d_a and d_0 are the d spacing of bulk and TiO_2 thin film from JCPDS data. Residual stress is classified into two: a) tensile stress is the stress that can be applied to an object by pulling on it, or attempting to stretch it. Positive values of stress indicate tensile stress. b) compressive stress is the stress applied to materials resulting to their compaction (decrease of volume). Negative values of stress indicate compressive stress.

The calculated residual stress are summarized in Table – 1 and 2 and shows the presence of both tensile and compressive stress in the prepared TiO_2 thin film with respect to their orientations. It is also noticed that the annealing temperature also influences the stress in the TiO_2 crystal. Table – 1 shows the change in residual stress for TiO_2 thin film deposited on glass substrates with respect to their growth orientations. On the preferred (111) orientations, the tensile stress are developed and increased at high annealing temperature. On comparison, tetragonal has low residual stress than orthorhombic phase. The residual studies are also extended for TiO_2 thin film deposited on Al substrate and the calculated results are given in table – 2. It clearly shows that a noticeable change in residual stress could be observed as the annealing temperature increases. From table – 2, it is clearly understood that the residual stress decreases as the annealing temperature increases and a transformation from compressive to tensile is also observed for the film annealed at 100 °C for (110), (112) and (121) orientations. As compared to the glass substrates, compressive stress is dominated with low value at high annealing temperature for TiO_2 thin film where as high tensile stress are possible with glass substrates. Overall, it is clearly understood that the substrates decides the film quality especially the residual stress developed during the growth.

Table 2. Structural properties of TiO_2 *thin film on Al substrates for various annealing temperatures.*

2θ (O)	2 θ (S)	FWHM	*d* space (O)	*d* space (S)	Residual stress	Phase
Room Temperature (25°)						
34.73	34.75	0.0787	2.582	2.579	-0.29703	R
38.57	38.57	0.0787	2.335	2.333	-0.17579	T
40.31	40.36	0.1181	2.238	2.2329	-0.43709	O
53.27	53.89	0.1200	1.718	1.700	-2.38607	T
58.27	58.48	0.0960	1.582	1.577	-0.19269	O
62.15	62.11	0.1200	1.492	1.493	0.016095	T
65.17	65.27	0.0960	1.430	1.428	-0.33561	T
69.59	69	0.1440	1.349	1.359	1.537057	T
78.54	78.65	0.0960	1.219	1.215	-0.23744	T
100°C						
34.79	34.75	0.0590	2.578	2.579	0.032692	R
38.64	38.57	0.0787	2.335	2.333	0.063195	T
40.37	40.36	0.1181	2.238	2.2329	0.010486	O
53.33	53.89	0.0720	1.716	1.700	-0.1765	T
58.33	58.48	0.0960	1.582	1.577	-0.03563	O
62.21	62.11	0.0960	1.491	1.493	0.018423	T
65.23	65.27	0.0960	1.430	1.428	-0.00757	T
69.65	69	0.1200	1.349	1.359	0.07457	T
78.60	78.65	0.0960	1.219	1.215	-0.03123	T
200°C						
34.71	34.75	0.0787	2.584	2.579	-0.01605	R
38.65	38.57	0.0787	2.335	2.333	-0.0085	T
40.32	40.36	0.1181	2.238	2.2329	-0.01614	O
53.24	53.89	0.1200	1.718	1.700	-0.07547	T
58.25	58.48	0.0960	1.582	1.577	-0.02197	O
62.15	62.11	0.1200	1.492	1.493	0.002196	T
65.17	65.27	0.0960	1.430	1.428	-0.00897	T
69.59	69	0.1200	1.349	1.359	0.035783	T
78.58	78.65	0.0960	1.219	1.215	-0.02035	T
300°C						
38.57	38.57	0.0787	2.335	2.333	-0.0038	T
65.18	65.27	0.0960	1.430	1.428	-0.00608	T
78.54	78.65	0.0960	1.219	1.215	-0.01532	T
400°C						
25.41	25.36	0.2755	3.508	3.509	0.00069	T
38.55	38.57	0.0787	2.335	2.333	-0.00298	T
65.16	65.27	0.0960	1.430	1.428	-0.00481	T
78.56	78.65	0.0960	1.219	1.215	-0.01212	T

(O) – observed, (S) – Standard

4. Conclusion

TiO_2 thin films were deposited on glass and Al substrates using RF sputtering and confirmed the formation of mixed phases on both substrates by XRD analysis. The microstructural parameters were evaluated from the XRD spectra and showed a noticeable changes when the film annealed at different temperatures. Tetragonal phases were noticed for Al substrates whereas the orthogonal phase was observed on glass substrates at high annealing temperatures. Preferred growth of tetragonal phases was confirmed on Al substrates at high annealing temperatures by texture coefficient analysis. The annealing temperature showed an immense effect on the change in structural parameters of TiO_2 thin film especially at 100°C. The observed crystallite size lied in between 60 and 140 nm. The prepared TiO_2 thin film on glass substrates were tensile nature whereas it was compressive nature when deposited on Al substrates.

Acknowledgements

We would like to acknowledge the NOR lab, school of physics to provide the rf sputtering and other facility for this study.

References

[1] B. Guo, Z. Liu, L. Hong, H. Jiang, J. Yang-Lee, Thin Solid Films, **479**, 310 (2005).
[2] D. Mardare, E. Apostol, J. Optoelectron. Adv. Mater. **8**(3), 914 (2006).
[3] A. CondeGalardo, M. Garcia Rocha, I. Hernandez –Calderon, R. Palomino-Merino, Appl.Phy. Lett. **78**(22), 3436 (2001).
[4] R. Palomino-Merino, A. CondeGalardo, M. Garcia-Rocha, I. Hernandez –Calderon, V. Castano, R.Rodriguez, Thin Solid Films **401**, 118 (2001).
[5] Zeman P, Takabayashi S. Thin Solid Films, **433**,57 (2003)
[6] W. Zhou, X. Zhong, X. Wu, L. Yuan, Q. Shu and Y. Xia, J.Korean Phy.Soci., **49**(5), 2168 (2006).
[7] P.R. Mishra, P.K. Shukla, O.N. Srivastava, Int. J. Hydrogen Energy, **32**, 1680 (2007)

[8] M.G. Kang, N.G. Park, K.S. Ryu, S.H. Chang, K.J. Kim, Sol. Energy Mater. Sol. Cells, 90574 (2006).
[9] A. Maloney, E.L. Schoonman, J. Chem. Vapor. Depos.,**4**, 109 (1998).
[10] J.Krzak-Roś, J.Filipiak, C. Pezowicz,A.Baszczuk, M. Miller, M. Kowalski, R.Będzińsk,Acta of Bioengg.andBiomech.,**11**(2), 21 2009.
[11] P.Suna, H.Liub, H. Yanga, W.Fua, S.Liua, M. Lia,Y.Suia, Y.Zhanga, Y. Li, Appl. Surf. Sci. **256**, 3170 (2010).
[12] A.H.Mayabadi, V.S.Waman, M.M.Kamble, S.S.Ghosh , B.B.Gabhale, S.R.Rondiya, A.V.Rokade, S.S.Khadtare, V.G.Sathe, H.M.Pathan, S.W.Gosavi, S.R.Jadkar, J.Phy.Chem Solids, **75**, 182 (2014).
[13] H. Kikuchi, M. Kitano, M. Takeuchi, M. Matsuoka, M. Anpo, P. V. Kamat, J.Phy. Chem. B **110**, 5537 (2006).
[14] N. S.Begum and H. M.Farveez Ahmed, Bull. Mater. Sci., **31**(1), 43 (2008).
[15] M. Stamate, G. Lazar, I. Lazar, Rom. Journ. Phys., **53**(1–2), 217 (2008)
[16] http://202.120.223.158/download/26da9cdf-6134-41fc-bf56-6dcccd9edd20.pdf
[17] B.D. Cullity, In: *Elements of X-Ray Diffraction*. 2nd edition. Cohen M, editor. Reading, Mass, USA: Addison-Wesley; 1978.
[18] C. Mehta, J. Abass ,G. Saini, S. Tripathi, Chalcoge.Lett., **11**, 133 (2007)
[19] F.H. Chung, D.K. Smith, Industrial applications of X-ray diffraction. New York: Marcel Dekker; 1999. p. 798.
[20] H. Hadouda, J. Pouzet, J. C. Bernede, A. Barreau, Mat. Chem.Phys. **42**, 291 (1995)
[21] A. J. Perry, J. Vac. Sci. Technol. **A8**, 1351 (1990).
[22] L. Borgese, M. Gelfi, E. Bontempi, P. Goudeau, G. Geandier, D. Thiaudière, L.E. Depero, Surf.Coat., Tech.,**206**, 2459 (2012).